High-amplitude time reversal focusing of airborne ultrasound to generate a focused nonlinear difference frequency

Carla B. Wallace, and Brian E. Anderson

Citation: The Journal of the Acoustical Society of America **150**, 1411 (2021); doi: 10.1121/10.0005907
View online: https://doi.org/10.1121/10.0005907
View Table of Contents: https://asa.scitation.org/toc/jas/150/2
Published by the Acoustical Society of America

JASA ARTICLE

High-amplitude time reversal focusing of airborne ultrasound to generate a focused nonlinear difference frequency

Carla B. Wallace and Brian E. Anderson[a)]
Acoustics Research Group, Department of Physics and Astronomy, Brigham Young University, N283 Eyring Science Center, Provo, Utah 84602, USA

ABSTRACT:
Time reversal (TR) focusing of airborne ultrasound in a room is demonstrated. Various methods are employed to increase the amplitude of the focus. These methods include creating a small wooden box (or chamber) to act as a miniature reverberation chamber, using multiple sources, and using the clipping processing method. The use of a beam blocker to make the sources more omnidirectional is also examined, and it is found that for most source/microphone orientations, the use of a beam blocker increases the amplitude of the focus. A high-amplitude focus of 134 dB peak re 20 μPa sound pressure level with a center frequency of about 38 kHz is generated using TR. Using four sources centered at 36.1 kHz and another four sources centered at 39.6 kHz, nonlinear difference frequency content centered at 3.5 kHz is observed in the focus signal. The difference frequency amplitude grows quadratically with increasing primary frequency amplitude. When using beam blockers, the difference frequency content propagates away from the focal location with higher amplitude than when beam blockers are not used. This is likely due to the differences in the directionality of the converging waves during TR focusing. © *2021 Acoustical Society of America.*
https://doi.org/10.1121/10.0005907
(Received 4 February 2021; revised 28 July 2021; accepted 30 July 2021; published online 25 August 2021)
[Editor: Julien de Rosny] Pages: 1411–1423

I. INTRODUCTION

Time reversal (TR) signal processing is a technique that can be used to focus acoustic wave energy to a point in space.[1,2] The method employs multiple sources and/or multiple reflections off walls in a room, which upon TR of the impulse response(s), are timed in such a way that the sound waves add constructively at a focal point within the room. During the so-called forward step of TR, an impulse response between a source located at point A in a room and a microphone at point B is obtained. If the impulse response is reversed in time and broadcast from point A (the so-called backward step of TR), the later reflections are broadcast first and then early reflections, and finally, the direct arrival is broadcast. Energy from each emission in the time-reversed impulse response (TRIR) arrive simultaneously at point B and constructively interfere to create a TR focus of sound. In truth, the emissions from the TRIR will travel many additional paths and arrive at point B at various times, creating artifacts in the waveform recorded at point B before and after the time of peak focusing, called side lobes.[3] Nevertheless, reverberant energy may be focused from one or more remotely placed sources to a selected location within a room.

The first known application of TR was signal transmission in the ocean in the 1960s,[4,5] though it was termed matched signal processing at the time. Candy *et al.*[6,7] and Meyer *et al.*[8] applied TR to audible frequency communications in a reverberant room, using audible sound in air.[6–8] Ribay *et al.* studied audible sound and TR focusing in a room with varying absorption and asserted that TR focal amplitude is proportional to the reverberation time of the room.[9] Denison and Anderson validated this relationship in the case that reverberation time changes as a result of a changing absorption coefficient in a fixed-sized room, but they showed numerically and experimentally that when reverberation time is a function of room size, a smaller room (with a shorter reverberation time) yields a higher focal amplitude.[10] Simpson and Anderson[11] used ultrasound in elastic media to also confirm the findings of Denison and Anderson. Willardson *et al.* created a high-amplitude focus of audible sound in air, where the peak pressure amplitude at the focus was 173.1 dB peak re 20 μPa. At these pressure levels, they observed nonlinear effects from the air, including high-frequency sound generation and waveform steepening.[12]

Applications of high-amplitude TR using ultrasound include nondestructive evaluation (characterizing cracks in solid materials),[13–17] lithotripsy for destroying kidney stones,[18,19] and treatment of brain tumors.[20,21] In all these applications, ultrasound is used in a solid or in the human body. Montaldo *et al.* used TR in a solid waveguide to create a high-amplitude focus of ultrasound with an intended application to lithotripsy of kidney stones.[18] They used one-bit TR, which increases the amplitude of the focus. They achieved amplitudes that were 15 times greater than when not using one-bit processing and asserted that the focal amplitude is proportional to the bandwidth of the transducer. Young *et al.* studied the effect of impulse response

[a)]Electronic mail: bea@byu.edu, ORCID: 0000-0003-0089-1715.

modification techniques (including one-bit processing) to increase TR focal amplitude, with an application to nondestructive crack detection.[22] Willardson *et al.* and Young *et al.* both found that clipping TR processing yielded higher amplitude focusing than one-bit TR.

A team led by Le Bas developed a noncontact source that generated ultrasound in a reverberant, air-filled cavity that interacted with a solid structure.[23–29] TR was used to focus energy efficiently within the air and in the structure, resulting in localized vibrations of the structure. Piezoelectric transducers generated ultrasound in air, and a laser Doppler vibrometer was used to measure impulse responses between the transducers' emissions and the structure's vibration. The laser vibrometer thus directly detected vibrations in the structure rather than acoustic pressures in the air. Some of this team's research explored focusing the ultrasound to a microphone location to see whether this focused ultrasound in air could excite vibration on the surface of any given structure; however, the most efficient TR focusing occurred when the vibration of the structure was used to measure the impulse responses. This Time Reversal Acoustic Non-Contact Excitation (TRANCE) source thus allows localized vibrational energy to be focused on the surface of a structure through coupling of ultrasound in air.

In summary, TR has been used with ultrasound in water, solids, and the human body as well as with audible sound in air. TR has also been used to focus ultrasound in air to generate localized vibration in a structure. These previous studies did not explore TR of ultrasound primarily with the intention to focus ultrasound in air or the potential nonlinear effects involved when that focusing is high in amplitude. The purpose of this paper is to demonstrate the use of TR to focus ultrasound in air to a point in space. Various methods are explored to optimize the amplitude of the TR focusing. The use of beam blockers is explored to create more omnidirectional sources. A comparison of omnidirectional sources (with the beam blockers in place) to directional sources (without the beam blockers) is made in relation to peak focal amplitude. It is then shown that TR can be used to generate a difference frequency at the focus. Potential applications of remotely focused, airborne ultrasound include selective microphone jamming, private communication, targeted pest deterrents, nonlethal weapons, and the creation of a "virtual" loudspeaker.

If high enough amplitudes are achieved in TR focusing of two different frequencies, it can create a difference frequency as a result of nonlinear propagation in the air itself, similar to the idea behind parametric arrays, which are discussed below. In such a case, it may be possible to create a spherically symmetric parametric array, which generates audible sound that propagates away from the focus location (by using two focused, primary ultrasonic signals at two different frequencies to generate a difference frequency). The idea of combining the parametric array with other ultrasonic applications, including TR, is mentioned briefly by Shi *et al.*,[30] but the implementation is not explored. Using two different frequencies to create a high-amplitude TR focus may create a virtual loudspeaker in the sense that audible sound seems to come from a location where no hardware is present. This would enable the creation of virtual sound sources within rooms, in locations where it may be difficult to place a traditional loudspeaker. Elaboration on the parametric acoustic array is included in the following paragraphs.

Parametric arrays have been developed to exploit nonlinear propagation of sound in air when high-amplitude sound at two different primary frequencies (f_1 and f_2) propagate in the same direction (collinearly).[31–33] "Collinear" means that the two primary frequencies travel in the same linear direction as each other. Nonlinear propagation produces sum and difference frequencies. The difference frequency $|f_1 - f_2|$ is of particular interest because this frequency can be audible while the primary frequencies are above the range of human hearing. There are commercially available parametric array loudspeakers (PALs) that generate audible difference frequency content. The difference frequency is highly directional because it is generated by the nonlinear mixing of ultrasonic frequencies as they propagate, forming a virtual end-fire array in the air.[31] The difference frequency initially becomes louder as the primaries propagate together until the point where the amplitudes of the primaries have significantly decreased due to atmospheric absorption and spherical spreading.[32] The audible difference frequency is independent from the primary frequencies in the sense that it continues to exist even after the primaries have died out.[33] The difference frequency beam inherits the directivity of the primary frequencies.

There is much debate in the literature concerning the theory on noncollinear interaction of sound with sound.[33–43] Although it seems undisputed that a difference frequency can exist within the interaction region of two primaries,[38,43] whether it is possible for the difference frequency to propagate away from the interaction region of noncollinear primary beams is contested.[33–43] Hamilton and TenCate specifically mentioned that local interaction of sound with sound, where the difference frequency does not necessarily propagate away from the region of interaction, may happen at the focus of converging waves.[43]

TR creates a focus of converging waves. During symmetric TR focusing, waves converge toward the focus location with spherical symmetry, constructive interference occurs, and then waves diverge with spherical symmetry.[44] Because the waves converge toward and then diverge away from the focal location, one can argue that two primary frequencies focused using TR propagate like collinear waves do for a parametric array. Thus, it seems that an outward propagating difference frequency can be created as long as primaries propagate with the same symmetry (they travel in the same direction as each other). Because the term collinear refers to one Cartesian direction, and spherically converging and diverging waves will be considered here, the phrase "shared propagation paths" will be used in place of "collinear" to describe two primaries that travel in the same direction. If the environment in which TR is performed is

https://doi.org/10.1121/10.0005907

not very reverberant, there may be only a couple of reflections that propagate toward the focus location from disparate directions. Thus, the two primaries might never travel with shared propagation paths, and the difference frequency generation may be limited to a local interaction in the focal region. The existence of the difference frequency away from the focal location, when focusing two primary frequencies, will be explored briefly in this paper.

Section II explains the experimental setup. This includes the use of a wooden box reverberation chamber, modification of the directivity of sources (using a beam blocker), equipment used, selection of frequencies used, design of transformers to use with amplifiers, an evaluation of distortion in the microphones used, and signal processing methods used. Section III presents experimental results. This includes the dependence of TR focal amplitude on the angle of the source(s) relative to the microphone, comparing both the blockers and no-blockers cases. Also included is the maximum focal amplitude achieved with eight sources. A difference frequency is observed when using four sources at one frequency band and four sources at another band. The dependence of the amplitude of this difference frequency on distance from the focal location greatly depends on whether beam blockers are used. Section IV discusses conclusions.

II. EXPERIMENTAL SETUP

A. Equipment and software

To perform the TR experiments in this paper, customized LabVIEW software (NI, Austin, TX) was used that interfaces with the signal generation and digitization cards. The software synchronizes the generation of eight arbitrary waveform signals and the digitization of four input signals. During the forward step in the experiments conducted for this study, rather than emitting an impulse from a source, the impulse response was obtained by broadcasting a chirp signal from each source individually, recording the chirp responses with a microphone, and calculating the band-limited impulse responses through a cross correlation of the chirp responses with the input chirp signal[45,46] (see Appendix C). TR processing techniques (such as one-bit TR or clipping TR) were then applied to the TRIR. Finally, during the backward step, the TRIR signals were broadcast from all sources simultaneously, and the TR focal signal was recorded. The same sampling frequency for both the generator and digitizer cards was used.

Two four-channel Spectrum M2i.6022 generator cards (14-bit resolution; Spectrum Instrumentation GmbH, Grosshandorf, Germany) and one four-channel Spectrum M2i.4931 digitizer card (16-bit resolution) were used for all measurements described here, except for the electrical impedance measurements. Two types of microphones were used: a 6.35-mm (1/4-in.) GRAS 40BE Free-Field Microphone with a 26CB preamplifier (GRAS Sound & Vibration, Holte, Denmark) and a 12.7-mm (1/2-in.) GRAS 46AQ Random Incidence Microphone Set. The 6.35-mm microphone was used for all measurements unless specified otherwise. The microphones were used with a GRAS 12AX 4 Channel CCP Power Module (GRAS Sound & Vibration). The ultrasonic sources used here were piezoelectric PAR4012A sources (Parsonics, Woodstock, IL) meant to be driven with frequencies near 40 kHz. For some measurements, the signal from the generator cards was amplified with 2350 Precision Power Amplifiers (with 50 times gain; TEGAM Inc., Geneva, OH) used in conjunction with direct current (DC) blocking capacitors and 4:1 transformers (see Appendix A). Some measurements did not use any amplification of the source signals.

B. Signal processing

Willardson *et al.* compared five signal processing methods that can be applied to a TRIR for audible sound in a room, namely traditional TR, clipping TR, one-bit TR, deconvolution TR, and decay compensation TR.[12] Clipping TR, one-bit TR, and decay compensation TR are methods that aim to increase the amplitude of the TR focusing, whereas deconvolution TR aims to provide a cleaner TR focusing signal. Of these five methods, they found that clipping yielded the highest amplitude TR focus. In clipping TR, the TRIR is normalized, and a threshold value is selected (0.01 was selected for these experiments). Amplitudes that are between a ratio of 0.01 and 1.0 times the peak amplitude of the impulse response are set equal to values of 0.01, whereas amplitudes between -0.01 and -1.0 times the peak amplitude of the impulse response are set equal to -0.01. This clipped TRIR is then normalized again, resulting in many values at ± 1.0. The principle is the same as that described by Derode *et al.*[47] for one-bit TR in that even though one-bit TR and clipping TR processing greatly distort the amplitude information in the TRIR, the critical phase information in the TRIR (or the timing of reflections) is preserved, allowing TR focusing to still occur. Because more energy is contained in the TRIR when using a clipping TR than in the unmodified TRIR, the amplitude of the TR focusing is greater. The key difference between one-bit TR and clipping TR is that in one-bit TR, the amplitudes are only set to either $+1$ or -1, essentially removing the smaller amplitudes within the TRIR, whereas in clipping TR, these smaller amplitudes are not zeroed out. Young *et al.* performed a similar analysis of these TRIR signal processing methods using ultrasonic elastic waves, yielding similar findings.[22] Based on these results, clipping TR was selected to modify the TRIR to create the highest amplitude TR focus possible. Higher amplitudes are more likely to allow a better chance of observing nonlinear sound propagation in the air during TR focusing. However, methods such as one-bit TR and clipping TR introduce distortion as a result of the signal processing (squaring off the tops of the signals).[22] This is necessary to consider if harmonic generation is of interest, but the distortions that are due to clipping will not produce a difference frequency. Therefore, if a difference frequency is seen in the signal, it came from a source of nonlinearity other than the clipping TR processing.

C. Miniature reverberation chamber

A small wooden box with a volume of 0.58 m^3 (internal dimensions 83 cm × 105 cm × 66 cm) was created to use as a miniature reverberation chamber [see Figs. 1(a)–1(c)]. The dimensions of the box were chosen to correspond to the golden ratio $2^{\frac{1}{3}} : 4^{\frac{1}{3}} : 1$; therefore, the room aspect ratio is identical to the simulations of Denison and Anderson.[10] The use of a smaller volume was motivated by Denison and Anderson's work, where they found that a smaller room size increases TR amplitudes with traditional TR (they did not study the effect of room size on TR amplitude with clipping TR). Because atmospheric absorption is a bigger factor at ultrasonic frequencies, this was another reason to conduct these experiments in a smaller volume box rather than a typical room. The box was made of 1.9-cm (3/4-in.) medium density fiberboard (MDF). Using reverse Schroeder integration,[48,49] the reverberation time of this box for the primary frequency bandwidth of 35.1–40.5 kHz was found to be 77 ms.

In a subsequent study, Denison and Anderson stated that for a TR process in a rectangular room, placing the sources and receivers in the same Cartesian plane increases focal amplitude.[50] Throughout the TR measurements reported here, the sources and receivers were placed at the same height in the wooden box. Denison and Anderson showed that TR focal amplitude increases somewhat as distance between source and microphone increases beyond the critical distance for the room. The critical distance r_c has been defined by many authors in room acoustics literature as

$$r_c = \sqrt{\frac{\gamma R}{16\pi}}, \tag{1}$$

where γ is the directivity factor of the sound source and R the room constant defined as

$$R = \frac{\langle \alpha \rangle_S S}{1 - \langle \alpha \rangle_S}, \tag{2}$$

where $\langle \alpha \rangle_S$ is the spatially averaged absorption coefficient of the walls in the room and S the surface area of the room. An approximate absorption coefficient of $\langle \alpha \rangle_S = 0.115$ for MDF was measured at 40 kHz by analyzing incident and reflected sound from a board placed in an anechoic chamber.[51] From this, the critical distance was estimated to be 10.5 cm (assuming $\gamma = 1$ for an omnidirectional source). Thus, for each TR experiment, the sources were placed at least 11 cm away from the microphone used for TR focusing. For the results in Sec. III, the sources were kept approximately 50 cm or farther from the microphone and approximately 10 cm or farther from the walls. The microphone used for the focusing was placed along an edge of this box, as recommended by Patchett *et al.*[52]

D. Source directivity

Because the wavelengths used (8.6 mm at 40 kHz) are small relative to the face of the transducers (radius, $a \approx 3.5$ cm; $ka = 22$, where k is the acoustic wavenumber), the sources are highly directional, which may not be desirable for exploiting reverberation to achieve high-amplitude TR focusing. Because TR relies on multiple reflective paths to create a focus, it is likely advantageous to make the sources more omnidirectional. Incidentally, the method suggested by Anderson *et al.*[46] to point the directional sources away from the focal location was attempted, but because the sources are so highly directional, this method proved detrimental to achieving a maximal TR focus amplitude when using the sources without beam blockers. To make the sources more omnidirectional, an aluminum disk with a small hole in the center (outside diameter, 10.2 cm; inside diameter, 8.1 mm; thickness, 3.05 mm) was placed in front of each source to act as a beam blocker to scatter the radiation. These disks were held in place with 3D-printed plastic holders designed to hold the disk 4.8 mm ± 1 mm away from the face of the source transducer [see Fig. 2(a)].

To choose the size of the blocker, measurements using a few different blocker sizes were performed. The outer diameter of the blocker and inner diameter of the blocker hole were explored briefly. Three different inner diameters of 12 mm, 8 mm, and 4 mm were achieved by taping washers of different sizes to the blocker disk (the 12-mm hole had no added washer). A 10-cm outer diameter blocker was used in all these different hole size cases. Three different outer diameters of blockers were then tested: 6 cm, 10 cm, and 13 cm (with the 8-mm washer in place to keep the inner diameter the same). For each change, a directivity measurement of the source/blocker configuration was taken, and the 40-kHz beam patterns were visually compared. All beam

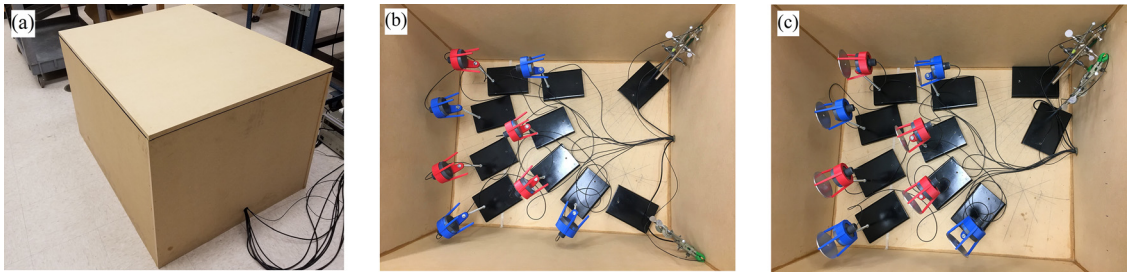

FIG. 1. (Color online) (a) Photograph of the 0.58-m^2 box used for the TR experiments. (b) and (c) Photographs of the interior of the box with the sources and the microphones visible. The sources are shown without and with beam blockers in (b) and (c), respectively. The focal location microphones are in the upper right corner of these images.

https://doi.org/10.1121/10.0005907

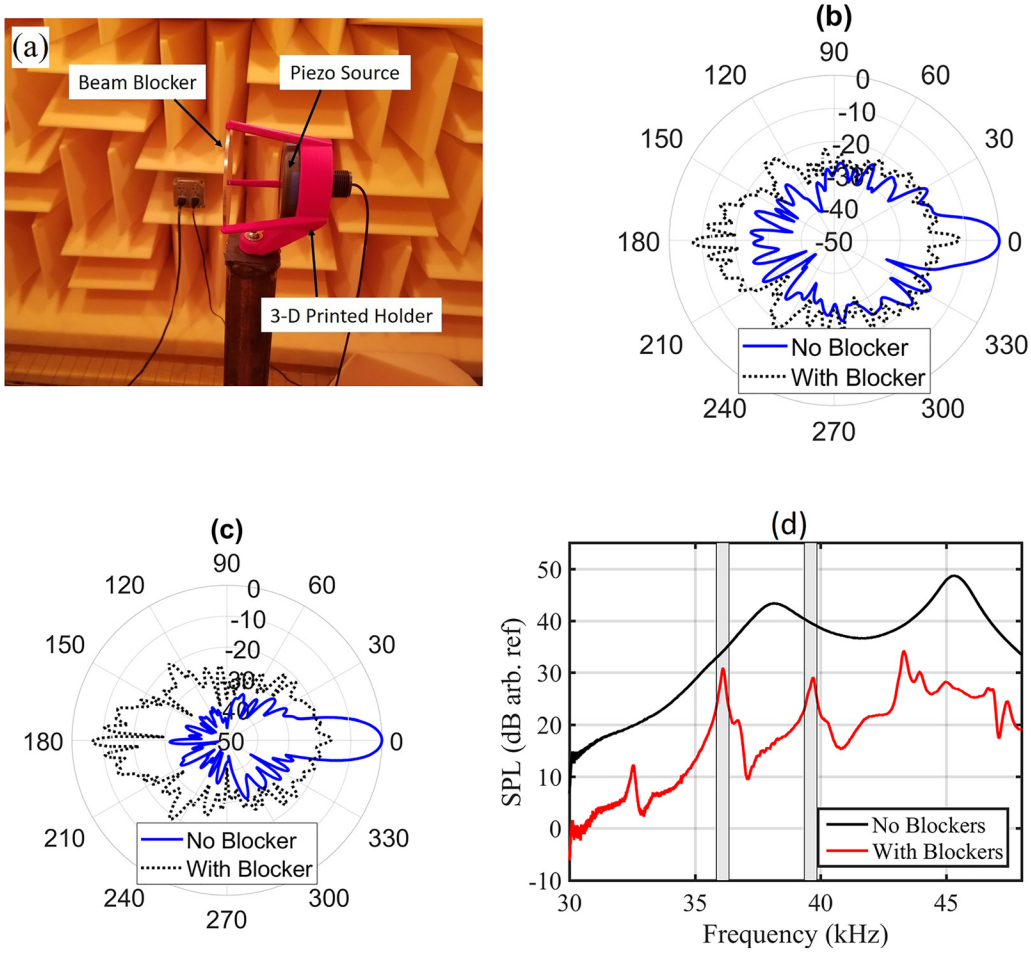

FIG. 2. (Color online) Photograph and beam patterns of an ultrasonic source. (a) Photograph of the source inside the 3D-printed holder, with a beam blocker. (b) and (c) Beam patterns with and without blockers (decibels relative to the no-blockers case at 0°) for 35.1–37.1-kHz bandwidth and 38.6–40.6-kHz bandwidth, respectively. (d) Average acoustic frequency response of eight piezoelectric sources at 0° relative to microphone, with and without the beam blockers present. The vertical gray bands represent the frequency bands used for the difference frequency generation experiments in Sec. III C. arb. ref, arbitrary reference units.

patterns were made with the same reference distance so that both the directionality and relative strength of the source could be compared for each configuration. Based on this visual comparison, it was decided to use a beam blocker with an outer diameter of 10 cm and an inner diameter of 8 mm. The frequency response of the sources was measured with the blockers in place, and it was found that the blockers introduce acoustic resonances. Seven standoff distances between the blocker and the face of the source were tested, and 4.8 cm was selected because the frequency response had two resonances that were fairly high amplitude, fairly equal to each other in amplitude, and within the acceptable frequency range (below 41 kHz to avoid the very low dip in impedance for these sources). Figures 2(b)–2(c) show the effect of the beam blocker on directivity for the two bandwidths (35.1–37.1 kHz and 38.6–40.6 kHz) chosen for the TR experiments.

The directivity measurements in the horizontal plane were also performed in the anechoic chamber as previously referenced. An ET250-3D Turntable (Outline Professional Audio, Flero, Italy) was used to make measurements every 1°. A metal stand was fabricated to mount the 3D-printed holders to the turntable (about 1 m tall). At each angle, a 35–46-kHz chirp was broadcast from the source and recorded with the 6.35-mm microphone. A sampling frequency of 5 MHz was used. The excitation signal contained a 500-ms long chirp signal. The spectrum at each angle was calculated, and at each frequency within the 2-kHz-wide bandwidths of interest, the amplitudes were squared and summed. This decibel value was referenced to the maximum value of the no-blockers case for the given bandwidth. Both the blockers and no-blocker case (for a given frequency bandwidth) thus had the same reference level.

Observation of the acoustic frequency response of the piezoelectric sources [see Fig. 2(d)] reveals that the beam blocker introduces its own acoustic resonances. (The beam blockers do not affect the electrical impedance of the sources.) The beam blocker is 4.8 cm away from the face of the source and creates the expected half-wavelength–multiple modes between the two nearly rigid boundaries (in the axial direction of the source). The bandwidths used here for TR experiments were centered on two of these new resonances (the 10th and 11th multiples of a half-wavelength mode based on a length of 4.8 cm) to achieve the highest TR

amplitudes possible. These two center frequencies, which correspond to the 10th and 11th mode frequencies, were 36.1 kHz and 39.6 kHz, respectively. These two resonance frequencies were selected to avoid frequencies at which the electrical impedance of the sources was too low (see Appendix A).

III. RESULTS

A. Effect of directivity on focal amplitudes

Anderson *et al.* showed that for somewhat directional sources in reverberant environments, the highest TR focal amplitude is achieved when the sources are pointed away from the microphone.[46] However, for highly directional sources, such as those used here, this is not the case, as was alluded to previously.

To determine the effect of highly directional sources on TR focal amplitudes, eight sources were used to create a TR focus. The peak focal amplitude was recorded for eight different angles of each source relative to the microphone focus location (0° means that all eight sources were pointed at the microphone, and the eight different angles are spaced every 45°). The results are shown in Fig. 3. A clipping threshold of 0.05 was used. Because Anderson *et al.* did not use clipping in their study,[46] the results reported in this paper are not directly comparable to their results. 800 mV were output directly from the card to the piezoelectric sources (no amplifier was used). A sampling frequency of 500 kHz was used, and the chirp was 100 ms long. The signals were bandpass filtered in the software, with a passband of 5–150 kHz to reduce noise in the signal. Ten averages were taken.

To determine the impact of the specific spatial locations of the sources within the box, error bars in Fig. 3 were estimated in the following way. Ten trials were performed (ten averages per trial), changing the position of the sources within the box for each new trial. Whenever the position of the sources was changed, the sources were always kept approximately 50 cm or farther from the microphone and approximately 10 cm or farther from the walls. For all these trials, the sources were pointed directly toward the microphone (0°). The forward chirp was centered on 36.1 kHz with a bandwidth of 2 kHz. The variation in level among different source placements, with all sources oriented at a 0° angle and with a bandwidth centered on 36.1 kHz, is assumed to be representative of the variation one would expect if the source positions were changed for all other angle orientations. This means that the error bars in the plots always reflect the variation in level due to different source positions only for the 0° angle orientations. The same error bars were used for the bandwidth centered on 39.6 kHz as well. For these ten trials, the experiment was performed both with the blockers in place and with no blockers. The error bounds in the figure at each angle are 1 standard deviation above and below the measured focal amplitude values.

The highest amplitude focus is generated when the sources are used with no blockers and are pointed directly at the microphone. However, when the sources are not pointed at the microphone, the highest amplitude focus is created when the sources are used with beam blockers. Thus, beam blockers provide an advantage for creating a higher amplitude focus at any selected location within the room for which the location would be at an arbitrary direction relative to the sources.

B. Peak levels of TR focusing

An effort was made to determine how large of a peak amplitude of TR focusing with ultrasound was possible using this setup. To do this, all eight sources were used in a TR experiment with blockers. Having each source emitting a bandwidth covering both resonances of the piezoelectric source–blocker setup was found to yield a higher peak amplitude (compared to bandwidths covering only one resonance); therefore, a chirp signal with a bandwidth from 35.1 kHz to 40.5 kHz was emitted from all eight sources during the forward step. The sources were pointed at 180° angles with respect to the focal location. A sampling frequency of 5 MHz was used to improve the resolution of the narrow focal peak. A forward chirp of 300 ms and clipping with a threshold of 0.01 were used. The generator cards

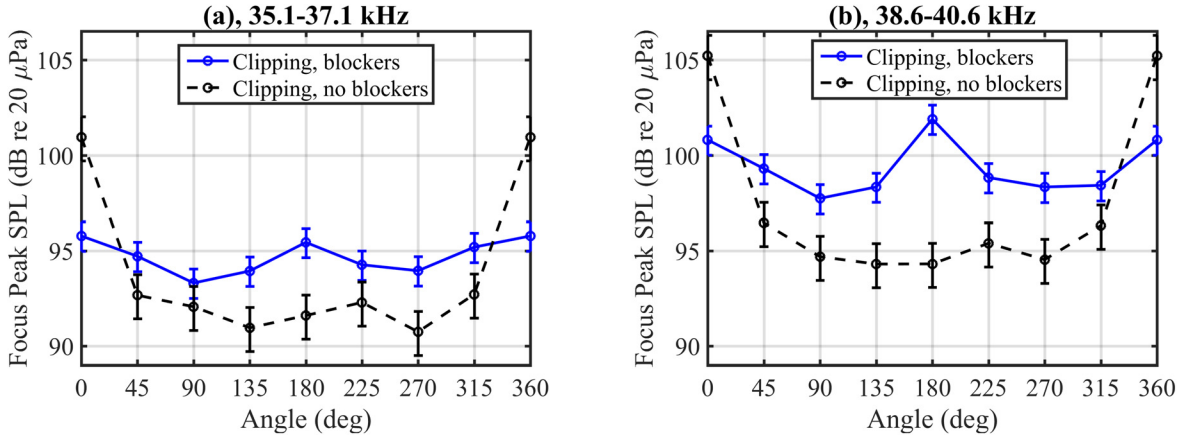

FIG. 3. (Color online) TR peak focal amplitude (reported as a peak SPL) for various angle orientations of eight sources with respect to the target microphone with and without blockers in place. Forward step chirp bandwidths are (a) 35.1–37.1 kHz and (b) 38.6–40.6 kHz. deg, degrees.

https://doi.org/10.1121/10.0005907

were used at their maximum voltage of ±3 V (which was then amplified, resulting in 18.8 V across the sources). Ten averages were taken. The peak focal amplitude in the TR focusing for this measurement was 134 dB re 20 μPa, with the peak frequency being at 39.5 kHz. This peak amplitude is higher than that achieved when the two sets of four sources emit the two different primary frequency bands.

Figure 4 displays the corresponding TR focal signal and the spectrum of this signal, as recorded by the 6.35-mm microphone. The peak pressure is 100 Pa (corresponding to the peak sound pressure level [SPL] of 134 dB re 20 μPa). The asymmetry of the signal is clearly evident and results from the use of clipping TR.[12] The two largest peaks in the spectrum correspond to the primary frequencies at about 35.9 kHz and 39.5 kHz. There are peaks at 3.6 kHz and 7.2 kHz resulting from some combination of microphone distortion (see Appendix B) and nonlinear acoustic mixing of the primaries (self-interaction). Side bands on either side of the primary peaks are also apparent. Note that the spectrum is a narrowband spectrum (Fourier transform over the entire focal signal), and some smoothing of this spectrum was implemented for better visual clarity of features within the spectrum.

C. Nonlinear difference frequency generation

To generate a difference frequency within TR focusing, the emission from four sources were centered on 36.1 kHz, and the emission from another four sources was centered on 39.6 kHz. A bandwidth of 500 Hz centered on each of these frequencies was used. The gray-colored bands in Fig. 2(d) denote the span of these primary frequency bands. Separate amplifiers were used for each frequency bandwidth to avoid crosstalk of the two bandwidths within the amplifier. Fifty averages were used on the backward step to decrease noise in the measurement. A 300-ms chirp with a sampling frequency of 500 kHz was used. Clipping TR was also used, with a threshold of 0.01. The amplitude of the primary frequency bands will always be reported using the 6.35-mm microphone because these microphones have a flat response that includes this frequency range. The amplitude of the difference frequency bans will always be reported using the 12.7-mm microphone because this microphone likely introduces less microphone distortion than the 6.35-mm microphone. Both sizes of microphone are placed end to end as discussed in Appendix B. When no beam blockers are used, the sources are pointed directly at the focal location (the target microphones). When the beam blockers are used, the sources are pointed 180° away from the focal location.

To determine whether the difference frequency content increased nonlinearly with respect to the primary frequency content, varying voltages were sent from the generator cards from 500 mV up to 3 V. The pressure spectra for the 3-V focal signals for each microphone are plotted in Figs. 5(a) and 5(b) for both the no-blockers case and the with-blockers case. The two primary frequencies are clearly visible as the two largest amplitude peaks in the spectra in Fig. 5(a). The peaks at the primary frequencies are higher in amplitude for the no-blockers case as expected. The peaks are also narrower for the with-blockers case likely because of the acoustic resonances between the blockers and the faces of the sources. The difference frequency at 3.5 kHz is visible for both cases and is higher in amplitude for the no-blockers case, which makes sense because the primary frequencies are higher in amplitude. A small peak at 7 kHz (twice the difference frequency) is also visible for the with-blockers case. Figure 5(b) shows more clearly the difference in the spectra for both cases around the difference frequency. Note that the background measurements were taken after the amplifiers were turned off, but input signals were still present in the wires, and potentially, some electromagnetic transmission occurred between cables at the primary frequencies for the 6.35-mm microphone [see Fig. 5(a)]. Even though the peak amplitude of the 3.5-kHz difference frequency in the spectrum recorded by the 6.35-mm microphone is higher than that recorded by the 12.7-mm microphone, we prefer to trust the amplitude obtained with the 12.7-mm microphone. The 12.7-mm microphone is much less sensitive to the primary frequencies and, thus, less susceptible to demodulation distortion (see Appendix B).

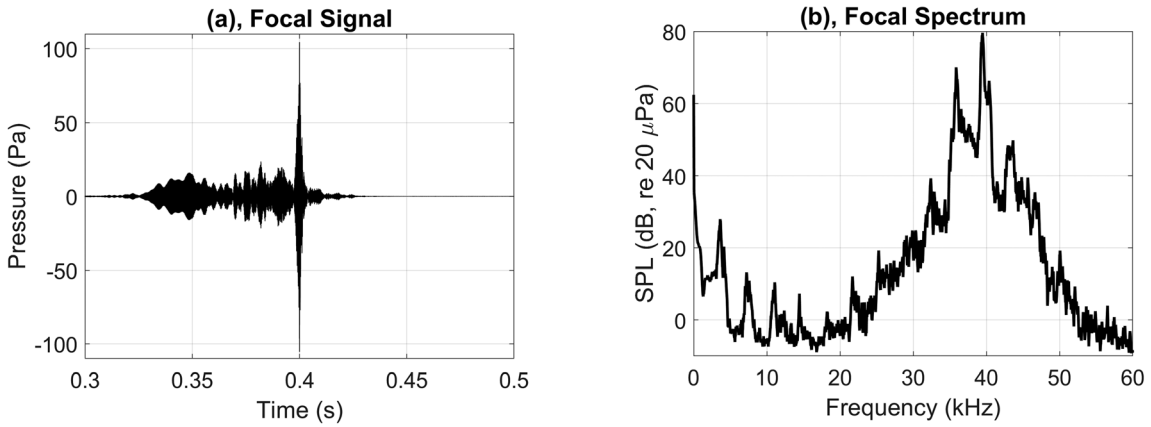

FIG. 4. (a) TR focal signal when using all eight sources and beam blockers, with the sources pointed 180° away from the focal location. (b) Spectrum of the focal signal in (a).

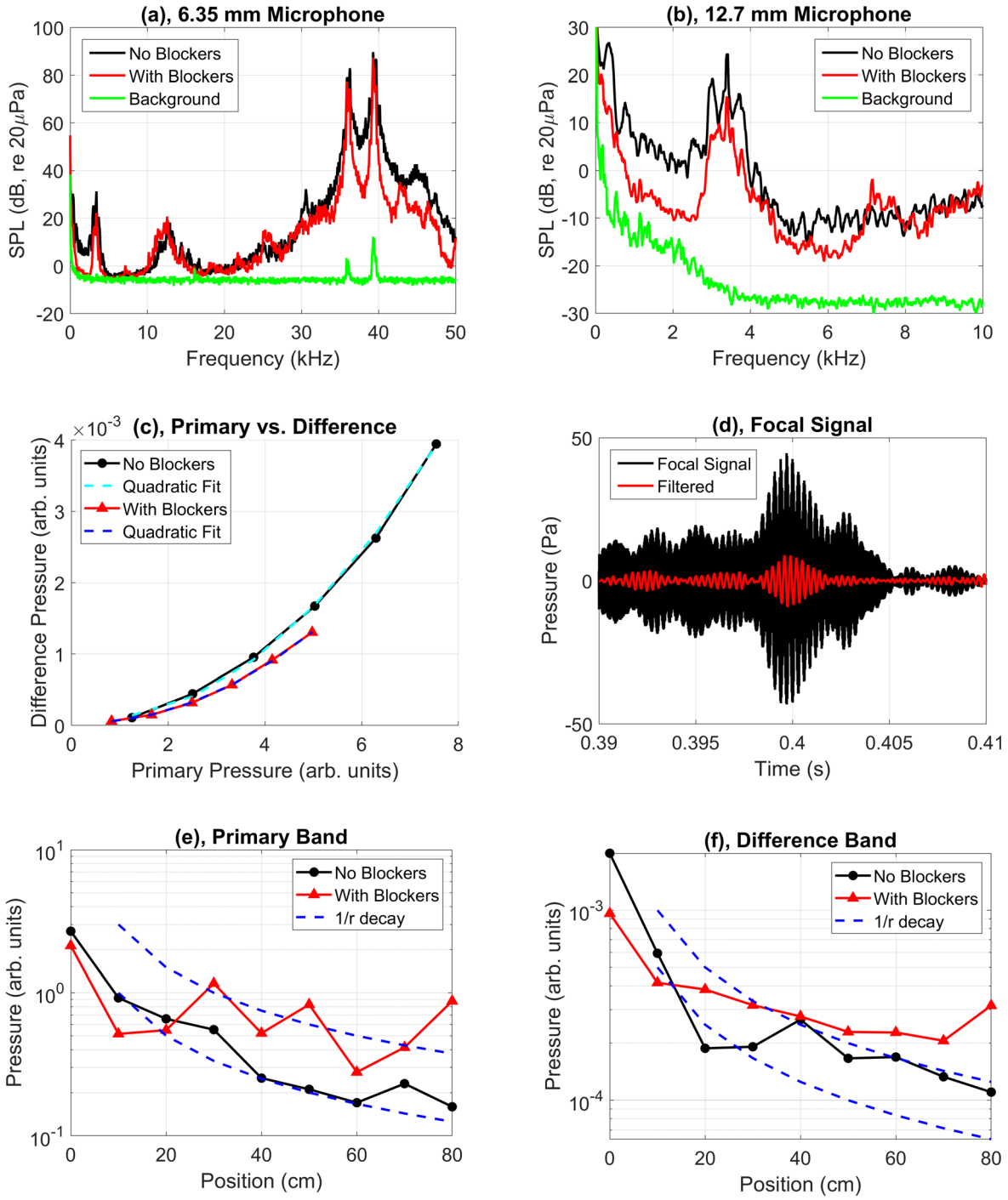

FIG. 5. (Color online) (a) Spectra of the unfiltered TR focus signal measured with the 6.35-mm microphone with and without the blockers present. (b) Spectra of the unfiltered TR focus signal measured with the 12.7-mm microphone with and without the blockers present. (c) Difference frequency equivalent pressure (3–4 kHz) vs primary frequency equivalent pressure (35–40 kHz) with and without blockers. Quadratic fits of data are shown by the dashed lines. (d) Sample unfiltered focus signal obtained with the blockers in place at the highest drive level while focusing both primary frequency bands. Also shown is a filtered focus signal (2–5 kHz) showing the difference frequency content multiplied by a factor of 500 for visualization purposes. (e) and (f) Equivalent pressure of the primary and difference frequency bands as a function of distance from the focal location. $1/r$ spherical spreading decay curves (blue dashed lines) are included for reference. arb., arbitrary.

To quantify an equivalent pressure amplitude for a particular frequency band of interest, the root mean square of the pressure amplitudes at each frequency bin within that band is determined:

$$p_{eq} = \sqrt{\sum p^2(f_i)}. \tag{3}$$

The equivalent SPL of this p_{eq} [equivalent $SPL = 20\log_{10}(p_{eq}/p_{ref})$, where $p_{ref} = 20\,\mu$Pa] may then be computed. The equivalent pressure for the difference frequency bandwidth from 3 kHz to 4 kHz is plotted against the equivalent pressure for the band spanning both primary frequencies (35–40 kHz) in Fig. 5(c). The data for both cases

https://doi.org/10.1121/10.0005907

show a quadratic dependence of the difference frequency equivalent pressure on the primary frequency equivalent pressure (the coefficient of determination R^2 for a quadratic fit to each of these datasets was approximately unity for both). A quadratic dependence is expected for a nonlinear parametric array.[31] This difference frequency generation may be the result of the high-amplitude primary frequencies interacting at the focal location, propagating together somewhat as they converge at the focal location. Without blockers, a larger equivalent pressure may be reached along with a correspondingly larger difference frequency equivalent pressure. It must be remembered that using no blockers only yields a larger focal amplitude when the sources are pointed directly at the intended focal location, whereas the sources with blockers in place yield a larger focal amplitude when the sources are pointed in other directions.

Figure 5(d) shows the focal signal, as measured by the 6.35-mm microphone, obtained for the with-blockers case with 18.8 V applied to the sources. The figure is zoomed in and does not fully show how asymmetric the focal signal is about the time of peak focusing [0.4 s, see Fig. 4(a)]; asymmetry of the focal signal is typical when using methods like clipping TR.[12] The focal signal measured by the collocated 12.7-mm microphone was bandpass filtered using an eighth order Butterworth filter, with cutoff frequencies of 2 and 5 kHz. This filtered signal was then multiplied by a factor of 500 to display it in Fig. 5(d). The oscillations visible for the filtered difference frequency band signal are at the period of the difference frequency. However, the actual oscillations of the primary frequencies in the unfiltered focal signal are so rapid over this time scale that one cannot see the individual cycles of the primary frequencies. Instead, what look like oscillations in the unfiltered focal signal are more like beat frequency oscillations.

When not using the beam blockers, the TR focusing is likely to be the result of converging waves that are more directional in nature. When the beam blockers are in place, the radiation from the sources is more omnidirectional. Thus, one might expect that the TR focusing when using beam blockers would more likely be the result of converging omnidirectional (spherical) waves. Measurements were made to determine how the primary frequency and the difference frequency vary with distance away from the focal location. Two pairs of 6.35- and 12.7-mm microphones were used. One pair was left at the focal location while the other was moved along one wall up to 80 cm away from the focal location (in a direction that did not correspond to moving directly toward any of the sources). The placement of the focal location microphones (in the upper right corner of the image) along with the source locations for the no-blockers case is visible in Fig. 1(b). The pair of microphones that were moved along the wall 80 cm away from the focal location (referred to here as the away microphones) are visible in the lower right corner of the image. Figure 1(c) displays the sources with blockers and their 180° orientation with respect to the focal location, and in this image, the away microphones are placed only 10 cm away from the focal location. The equivalent pressure of the primary frequency band (spanning 35–40 kHz) as a function of distance from the focal location for both blocker cases is shown in Fig. 5(e), while the equivalent pressure of the difference frequency band (spanning 3–4 kHz) vs distance for the two cases is shown in Fig. 5(f). In an effort to track only the difference frequency generation at the focal location and its subsequent propagation away from the focal location, the time included in the Fourier transform to calculate the primary and difference frequency bands was reduced. Only the time spanning the start of the main focal pulse [0.398 s, refer to Fig. 5(d)] to the expected time that the end of the focal pulse would arrive at the farthest away microphone position [0.403 s, refer to Fig. 5(d)] was included. Note that the background noise levels are at least an order of magnitude below the amplitudes plotted in Figs. 5(e) and 5(f).

Even though the amplitude of the primaries and the difference frequency is larger for the no-blockers case at the focal location, the amplitude of both of these drops off faster with increasing distance from the focal location for the no-blockers case. For the no-blockers case, the amplitude at the focal location for the primaries is 14 times larger than at the average of the 70-cm and 80-cm away locations, whereas the difference frequency drops off by a factor of 16. For the with-blockers case, the primaries are 3.3 times larger at the focal location than at the average of the 70-cm and 80-cm away locations, whereas the difference frequency drops off by a factor of 3.7. For spherical spreading decay of the sound pressure, an inverse relationship of pressure with distance from the source r should be expected. $1/r$ decay curves have been included on Figs. 5(e) and 5(f) for reference. It is apparent that the primary bands are decaying with distance at an approximate $1/r$ rate, except for the primary band with the beam blockers in the first 30 cm. However, the difference frequency band is falling off slower than the $1/r$ decay suggested by Westervelt.[31] The reason for this departure from spherical spreading is not known, but it could be caused by some diffuse field support from the room at the lower frequency difference band where the absorption of the walls would be less and, thus, the r_c would be shorter, indicating that a potential diffuse field effect could be more significant. Note that the authors measured the equivalent pressure amplitudes of the primary and difference frequency bands with and without the blockers present along a vertical spatial direction and found similar results [the results given in Figs. 5(e) and 5(f) were measured along a horizontal direction]. These results suggest that the more omnidirectional (spherical) the converging TR waves that arrive at the focal location are, the more the generated difference frequency can be expected to exist away from the focal location.

IV. CONCLUSION

TR of ultrasound in air has been demonstrated in a reverberant space. When using a highly directional source in a reverberant environment, the highest TR focal amplitude

is achieved when the sources are pointed directly at the focal location. However, the use of a beam blocker to make the sources more omnidirectional increases the focal amplitude for every other orientation of the sources relative to the focal location. Thus, the precise alignment of the sources with respect to any desired focal location is not necessary with the use of beam blockers. Clipping TR was used along with beam blockers in a miniature reverberation chamber to achieve a peak amplitude of 134 dB with airborne ultrasound, with a center frequency of 37.8 kHz. Small temperature fluctuations can significantly alter the time and amplitude of the TR focusing at ultrasonic frequencies, so the impulse responses should be recorded at the same conditions or be recorded shortly before the TR focusing step (see Appendix C).

Evidence of nonlinear difference frequency generation at the TR focus of high-amplitude ultrasound was observed. When using four sources at one frequency bandwidth and another four sources at a different bandwidth, a difference frequency at the focal location was recorded. The amplitude of the difference frequency varied quadratically with the amplitude of the primary frequency band. The degree to which this difference frequency is due to internal demodulation distortion in the motion of the microphone or to acoustic propagation nonlinear effects was not precisely determined here. Efforts were made to use a microphone less sensitive to the primary frequencies and, therefore, to decrease demodulation distortion within the microphones to more accurately measure the difference frequency caused by a parametric array-type effect. The amplitude of the difference frequency decreased less with distance from the focal location when using the beam blockers with the sources. This is likely due to the less directional nature of the TR focusing when using beam blockers.

ACKNOWLEDGMENTS

Funding provided by internal support from the Brigham Young University College of Physical and Mathematical Sciences is gratefully acknowledged. We thank Pierre-Yves Le Bas for developing software used early on in this project, Adam Kingsley for software that was used the most for this project, Brian Patchett for assisting with some measurements, and Jeremy Peterson and his assistants for making parts.

APPENDIX A: SOURCE OPTIMIZATION

The average measured electrical impedance of the eight sources used is shown in Fig. 6(a). At 45 kHz, the impedance dips to 80 Ω. This was problematic because the transducers draw too much current from the amplifiers. The TEGAM 2350 amplifiers had an output current limit of 40 mV. For an 80-Ω load, this only allowed an output of 3.2 V from the amplifier into the source before reaching the current limit. Thus, it was decided to avoid this piezoelectric resonance by staying below 41 kHz. Impedance measurements were taken using a MFIA Impedance Analyzer (Zurich Instruments, Zurich, Switzerland).

The impedance dips to approximately 350 Ω at 37 kHz. To handle this low impedance, eight transformers were made (one for each source). These transformers had a 4:1 winding ratio (P Core T-38 22×13 Ferrite 192×48 #30AWG; EPCOS AG, Munich, Germany), which increased the voltage allowed at the output of the amplifier while keeping the amplifier's output current at or below 40 mA. This increased the total possible power output from the amplifiers, allowing more power to be transferred to the piezoelectric source. With the transformers in place, an output voltage of 150 V from the amplifiers (with a 3-V input) was achieved. On the source side of the transformer, the voltage is reduced by a factor of 8 but the current is stepped up by a factor of 8; thus, the voltage across each source was 18.8 V when using a 3-V input to the amplifiers. Because these transformers had a very low (approximately 2.4 Ω) impedance for DC signals, a small offset of even 100 mV at the output of the amplifier would draw more than the amplifier's current limit of 40 mA. A 100-μF capacitor (that can handle up to 300 V of alternating current) was put in series with the transformer between the amplifier and transformer to block DC current. A diagram of the setup is shown in Fig. 6(b).

An experiment was performed using clipping TR with a threshold of 0.01. The sources were used with blockers in place, and sources were pointed 180° (away) from the target microphone. While using four of the sources centered at

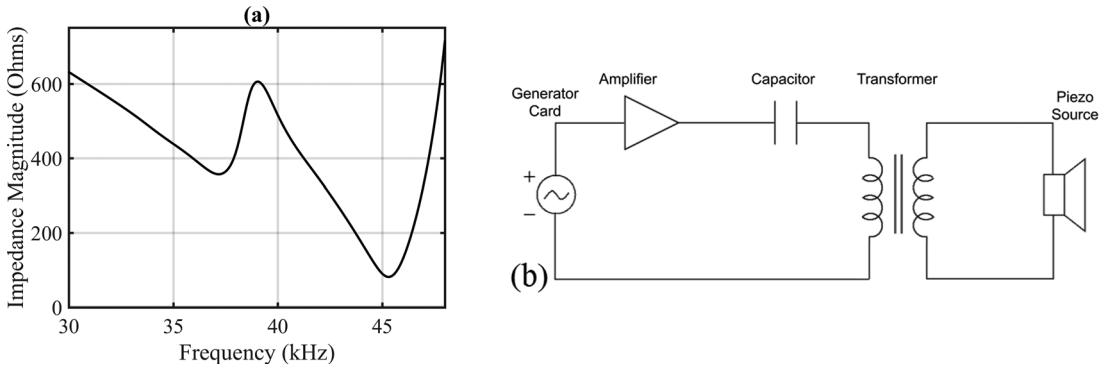

FIG. 6. (a) Average electrical impedance of the eight piezoelectric sources. (b) Setup diagram using generator card, amplifier (triangle), DC blocking capacitor, 4:1 transformer, and source.

https://doi.org/10.1121/10.0005907

36.1 kHz and the other four sources centered at 39.6 kHz, the bandwidth of both of the respective forward chirp signals were incrementally changed to find an optimal bandwidth of these ultrasound primary frequencies to generate the largest amplitude difference frequency possible. It was determined that a minimum bandwidth of 500 Hz for each primary yielded the largest overall amplitude TR focusing. In addition, a bandwidth less than 1 kHz for each primary yielded the largest difference frequency amplitude in the TR focusing. Thus, a bandwidth of 500 Hz for each primary frequency band was selected to generate the difference frequency. These primary bandwidths are identified in Fig. 2(d) by the gray-colored vertical bands. Because a difference frequency bandwidth centered on 3.5 kHz is expected, the bandwidth of the emitted chirps should be lower than 3.5 kHz. Otherwise, the difference frequency may be generated as a result of nonlinearities from self-interactions within an individual source's bandwidth. A narrow bandwidth is also advantageous because it should create a more clearly defined difference frequency in a frequency spectrum. Therefore, a balance should be found between the larger amplitudes offered by a large bandwidth and the clarity offered by a narrow bandwidth.

APPENDIX B: MICROPHONE NONLINEARITY

It is possible to record a difference frequency of two primary frequencies, even if the parametric array effect is not present. This can be due to distortions in the mechanical response of the microphone or in its circuitry.[32,53–55] Several researchers have distinguished between microphone nonlinearities and in-air demodulation by measuring the propagation curve of the on-axis difference frequency signal while varying the distance of the microphone from a parametric array loudspeaker (PAL) to observe departures from theory.[32,54]

To compare the two microphones' responses in detecting a difference frequency, the difference frequency of a PAL (HSS H450 Directed Audio Sound System; Turtle Beach Corporation; Bouaye, France) was measured at two distances from the PAL. Two microphones were placed end to end such that the grid caps of the microphones were touching [see Fig. 7(a)]. They were then moved to two different observation distances from the PAL as a 1-kHz signal was sent to the PAL (the PAL does the signal processing required to create this 1-kHz difference frequency using ultrasonic primary frequencies). At each of the two microphone positions, the voltage sent to the PAL was varied. The signals from each microphone could then be compared to the other. If the pressure amplitudes were different for each microphone, it was an indication of the presence of microphone distortion in at least one of the microphones. To ensure that the microphones were calibrated correctly, they were used to measure a 1-kHz signal broadcast from an ordinary loudspeaker. While in their end-to-end configuration, the microphone calibrations, which had been previously measured, gave the same SPLs for each microphone (within a fraction of a decibel). Thus, the end-to-end configuration did not affect the microphones' ability to record a frequency of 1 kHz. When the PAL was used, it produced a few primary frequencies, including 41 kHz, 42 kHz, and 43 kHz. These high-amplitude primary frequencies produce a difference frequency of 1 kHz (in addition to a weaker 2-kHz signal). The comparison of the results at various measurement distances to the expected theory for a parametric array was inconclusive, meaning that some amount of microphone distortion could be an issue for one or both of the microphones.

At a distance of 28 cm from the PAL [Fig. 7(b)], the 1-kHz difference frequency amplitudes differ between the two microphones by about 6 dB, indicating microphone distortion in at least one microphone. At a distance of 211.5 cm from the PAL [Fig. 7(b)], the 1-kHz difference frequency signals lie almost exactly in the same place, indicating little microphone distortion for this distance. Because the 1-kHz difference frequency amplitude is higher in the 6.35-mm microphone than in the 12.7-mm microphone when the

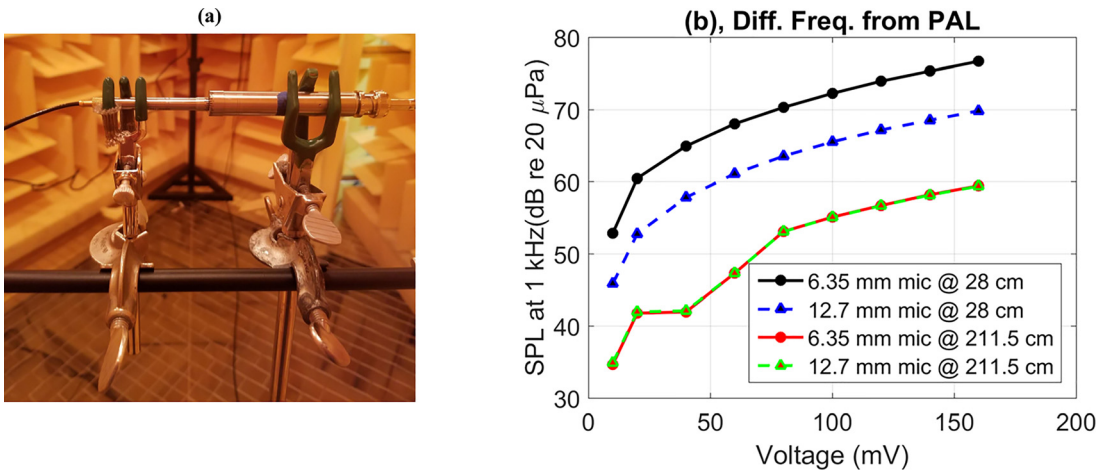

FIG. 7. (Color online) (a) Photograph of the configuration of two microphones end to end with grid caps touching. (b) Amplitudes recorded by two microphones 28 cm and 211.5 cm away from a PAL. Input voltage from the generator card to the PAL is varied. The 1-kHz signals recorded by both microphones lie almost exactly in the same place at the 211.5 cm distance. Diff. Freq., difference frequency; mic, microphone.

microphones are close to the PAL, it is assumed that the 6.35-mm microphone introduces more internal microphone distortion than the 12.7-mm microphone. This likely is attributable to the 12.7-mm microphone being much less sensitive to frequencies near 40 kHz, where the primaries are located, so there is less movement of the microphone diaphragm at these frequencies and less opportunity for demodulation distortion because of microphone movement (not acoustic nonlinearity in the air) to be introduced.

Thus, the 6.35-mm microphone is used to record the primary frequency amplitudes because its frequency range extends to these frequencies. The 6.35-mm microphone is not used to record the difference frequency amplitude because of the suspected microphone distortion. The 12.7-mm microphone is used to record the difference frequency amplitude. Because this microphone is far less sensitive to the primary frequencies, the microphone distortion should be significantly less, meaning that it may more accurately record the amplitude of the difference frequency.

APPENDIX C: TIME-VARYING IMPULSE RESPONSES

Often in audible-frequency TR experiments, the impulse response remains fairly constant throughout the course of several experiments, and the impulse response can be used for many backward steps of TR without needing to remeasure the impulse response. However, it was found that for this setup with ultrasound in air, the amplitude and time of focus shifted as time passed if an old impulse response was used. For one such trial, the impulse response was found, and then the backward step was performed repeatedly throughout the course of 43 min with that same reversed impulse response. Throughout this time, the peak pressure at the focus decreased with each subsequent recording and arrived earlier in time. After the 43 min, the peak pressure amplitude had shifted down by 10.9%, and the focus peak arrived 2.2 μs earlier than the focus peak measured at time 0. When the impulse response was remeasured before each backward step, the focal amplitude and arrival times were very consistent between measurements. For these trials, a sampling frequency of 5 MHz was used to capture the narrow focus peak with high resolution. A clipping threshold of 0.01, ten averages, a 2-kHz bandwidth (centered on 35.1 kHz for four sources and 39.6 kHz for the other four sources), and a 0.5-s chirp were used.

These two effects (lowering focal amplitude and shifting earlier in time) are likely due to small increases in temperature inside the box as time went on. Because sound speed increases as the square root of temperature, an increase in temperature would explain the slightly earlier arrival of the focus. Furthermore, because the time it takes to traverse the various path lengths changes less for shorter paths than it does for longer paths, the various broadcasts from the TRIRs no longer arrive at the focus at exactly the same time as one another, and the amplitude of the focus is lowered because of the slight staggering in time of the arrivals. The temperature in the room in which the wooden chamber is located is known to typically increase by about 2 °C from the morning until the afternoon (the temperature is not regulated well in this room). This presents a potential weakness of ultrasonic TR in a room: The impulse response can be affected by small changes in air temperature. Thus, when using TR of airborne ultrasound in larger rooms, it becomes more important for the impulse response to be obtained shortly before using it for TR, unless the temperature of the room is quite constant. These findings are related to the findings of Griffa *et al.*[56] and Scalerandi *et al.*[57] For the experiments presented in this paper, other than those in this appendix, the forward step of TR to obtain the impulse response was always repeated for each new TR-focusing experiment.

[1]M. Fink, "Time reversed acoustics," Phys. Today **50**(3), 34–40 (1997).
[2]B. E. Anderson, M. Griffa, C. Larmat, T. J. Ulrich, and P. A. Johnson, "Time reversal," Acoust. Today **4**(1), 5–16 (2008).
[3]C. Draeger, J.-C. Aime, and M. Fink, "One-channel time reversal in chaotic cavities: Experimental results," J. Acoust. Soc. Am. **105**(2), 618–625 (1999).
[4]A. Parvulescu and C. S. Clay, "Reproducibility of signal transmissions in the ocean," Radio Elec. Eng. **29**(4), 223–228 (1965).
[5]C. S. Clay and B. Anderson, "Matched signals: The beginnings of time reversal," Proc. Mtgs. Acoust. **12**(1), 055001 (2011).
[6]J. V. Candy, A. W. Meyer, A. J. Poggio, and B. L. Guidry, "Time-reversal processing for an acoustic communications experiment in a highly reverberant environment," J. Acoust. Soc. Am. **115**(4), 1621–1631 (2004).
[7]J. V. Candy, A. J. Poggio, D. H. Chambers, B. L. Guidry, C. L. Robbins, and C. A. Kent, "Multichannel time-reversal processing for acoustic communications in a highly reverberant environment," J. Acoust. Soc. Am. **118**(4), 2339–2354 (2005).
[8]A. W. Meyer, J. V. Candy, and A. J. Poggio, *Time Reversal Signal Processing in Communications—a Feasibility Study* (Lawrence Livermore National Laboratory Library, Livermore, CA, 2002).
[9]G. Ribay, J. de Rosny, and M. Fink, "Time reversal of noise sources in a reverberation room," J. Acoust. Soc. Am. **117**(5), 2866–2872 (2005).
[10]M. H. Denison and B. E. Anderson, "Time reversal acoustics applied to rooms of various reverberation times," J. Acoust. Soc. Am. **144**(6), 3055–3066 (2018).
[11]P. E. Simpson and B. E. Anderson, "The performance of time reversal in elastic chaotic cavities as a function of volume and geometric shape of the cavity," J. Acoust. Soc. Am. **150**(1), 526–539 (2021).
[12]M. L. Willardson, B. E. Anderson, S. M. Young, M. H. Denison, and B. D. Patchett, "Time reversal focusing of high amplitude sound in a reverberation chamber," J. Acoust. Soc. Am. **143**(2), 696–705 (2018).
[13]C. Prada, E. Kerbrat, D. Cassereau, and M. Fink, "Time reversal techniques in ultrasonic nondestructive testing of scattering media," Inv. Prob. **18**(6), 1761–1773 (2002).
[14]B. E. Anderson, L. Pieczonka, M. C. Remillieux, T. J. Ulrich, and P.-Y. Le Bas, "Stress corrosion crack depth investigation using the time reversed elastic nonlinearity diagnostic," J. Acoust. Soc. Am. **141**(1), EL76–EL81 (2017).
[15]S. M. Young, B. E. Anderson, S. M. Hogg, P.-Y. Le Bas, and M. C. Remillieux, "Nonlinearity from stress corrosion cracking as a function of chloride exposure time using the time reversed elastic nonlinearity diagnostic," J. Acoust. Soc. Am. **145**(1), 382–391 (2019).
[16]B. E. Anderson, M. C. Remillieux, P.-Y. Le Bas, and T. J. Ulrich, "Time reversal techniques," in *Nonlinear Ultrasonic and Vibro-Acoustical Techniques for Nondestructive Evaluation*, edited by T. Kundu (Springer International Publishing, Cham, Switzerland, 2019), pp. 547–581.
[17]N. Smagin, A. Trifonov, O. Bou Matar, and V. V. Aleshin, "Local damage detection by nonlinear coda wave interferometry combined with time reversal," Ultrasonics **108**, 106226 (2020).
[18]G. Montaldo, P. Roux, A. Derode, C. Negreira, and M. Fink, "Ultrasound shock wave generator with one-bit time reversal in a dispersive medium, application to lithotripsy," Appl. Phys. Lett. **80**(5), 897–899 (2002).

[19]J.-L. Thomas, F. Wu, and M. Fink, "Time reversal focusing applied to lithotripsy," Ultrason. Imaging **18**(2), 106–121 (1996).
[20]J.-L. Thomas and M. Fink, "Ultrasonic beam focusing through tissue inhomogeneities with a time reversal mirror: Application to transskull therapy," IEEE Trans. Ultrason. Ferr. Freq. Contr. **43**(6), 1122–1129 (1996).
[21]M. Tanter, J.-L. Thomas, and M. Fink, "Focusing and steering through absorbing and aberrating layers: Application to ultrasonic propagation through the skull," J. Acoust. Soc. Am. **103**(5), 2403–2410 (1998).
[22]S. M. Young, B. E. Anderson, M. L. Willardson, P. E. Simpson, and P.-Y. Le Bas, "A comparison of impulse response modification techniques for time reversal with application to crack detection," J. Acoust. Soc. Am. **145**(5), 3195–3207 (2019).
[23]P.-Y. Le Bas, T. J. Ulrich, B. E. Anderson, and J. J. Esplin, "Toward a high power non-contact acoustic source using time reversal," Acoust. Soc. Am. ECHOES Newslett. **22**(3), 7–8 (2012).
[24]S. Delrue, P.-Y. Le Bas, T. J. Ulrich, B. Anderson, and K. Van Den Abeele, "First simulations of the candy can concept for high amplitude non-contact excitation," Proc. Mtgs. Acoust. **16**, 045019 (2012).
[25]B. E. Anderson, T. J. Ulrich, and P.-Y. Le Bas, "Improving the focal quality of the time reversal acoustic noncontact source using a deconvolution operation," Proc. Mtgs. Acoust. **19**, 030080 (2013).
[26]P.-Y. Le Bas, T. J. Ulrich, B. E. Anderson, and J. J. Esplin, "A high amplitude, time reversal acoustic non-contact excitation (TRANCE)," J. Acoust. Soc. Am. **134**(1), EL52–EL56 (2013).
[27]S. Delrue, K. Van Den Abeele, P.-Y. Le Bas, T. J. Ulrich, and B. Anderson, "Simulations of a high amplitude air coupled source based on time reversal," in Proceedings of the International Congress on Ultrasonics, 2–5 May 2013, pp. 591–596.
[28]M. C. Remillieux, B. E. Anderson, T. J. Ulrich, P.-Y. L. Bas, M. R. Haberman, and J. Zhu, "Review of air-coupled transduction for nondestructive testing and evaluation," Acoust. Today **10**(3), 36–45 (2014).
[29]P.-Y. Le Bas, M. C. Remillieux, L. Pieczonka, J. A. Ten Cate, B. E. Anderson, and T. J. Ulrich, "Damage imaging in a laminated composite plate using an air-coupled time reversal mirror," Appl. Phys. Lett. **107**, 184102 (2015).
[30]C. Shi, Y. Kajikawa, and W. Gan, "An overview of directivity control methods of the parametric array loudspeaker," APSIPA Trans. Sig. Info. Proc. **3**, e20 (2014).
[31]P. J. Westervelt, "Parametric end-fire array," J. Acoust. Soc. Am. **32**(7), 934–935 (1960).
[32]M. B. Bennett and D. T. Blackstock, "Parametric array in air," J. Acoust. Soc. Am. **57**(3), 562–568 (1975).
[33]P. J. Westervelt, "Parametric acoustic array," J. Acoust. Soc. Am. **35**(4), 535–537 (1963).
[34]P. J. Westervelt, "Scattering of sound by sound," J. Acoust. Soc. Am. **29**(8), 934–935 (1957).
[35]U. Ingard and D. C. Pridmore-Brown, "Scattering of sound by sound," J. Acoust. Soc. Am. **28**(3), 367–369 (1956).
[36]J. L. S. Bellin and R. T. Beyer, "Scattering of sound by sound," J. Acoust. Soc. Am. **32**(3), 339–341 (1960).
[37]L. W. Dean, "Interactions between sound waves," J. Acoust. Soc. Am. **34**(8), 1039–1044 (1962).
[38]J. J. Truchard, "Parametric receiving array and the scattering of sound by sound," J. Acoust. Soc. Am. **64**(1), 280–285 (1978).
[39]J. A. TenCate, "Scattering of sound by sound: Nonlinear interaction of collinear and noncollinear sound beams," Ph.D. dissertation, Univ. of Texas, Austin, TX, 1992.
[40]P. J. Westervelt, "Answer to criticism of experiments on the scattering of sound by sound," J. Acoust. Soc. Am. **95**(5), 2865 (1994).
[41]P. J. Westervelt, "Answer to criticism of my treatment of nonscattering of sound by sound," J. Acoust. Soc. Am. **95**(5), 2865 (1994).
[42]P. J. Westervelt, "Scattering of sound by sound within the interaction zone," J. Acoust. Soc. Am. **96**(5), 3320 (1994).
[43]M. F. Hamilton and J. A. TenCate, "Sum and difference frequency generation due to noncollinear wave interaction in a rectangular duct," J. Acoust. Soc. Am. **81**(6), 1703–1712 (1987).
[44]B. E. Anderson, T. J. Ulrich, and P.-Y. Le Bas, "Comparison and visualization of focusing wave fields from various time reversal techniques in elastic media," J. Acoust. Soc. Am. **134**(6), EL527–EL533 (2013).
[45]B. Van Damme, K. Van Den Abeele, Y. Li, and O. Bou Matar, "Time reversed acoustics techniques for elastic imaging in reverberant and nonreverberant media: An experimental study of the chaotic cavity transducer concept," J. Appl. Phys. **109**(10), 104910 (2011).
[46]B. E. Anderson, M. Clemens, and M. L. Willardson, "The effect of transducer directivity on time reversal focusing," J. Acoust. Soc. Am. **142**(1), EL95–EL101 (2017).
[47]A. Derode, A. Tourin, and M. Fink, "Ultrasonic pulse compression with one-bit time reversal through multiple scattering," J. Appl. Phys. **85**(9), 6343–6352 (1999).
[48]M. R. Shroeder, "New method of measuring reverberation time," J. Acoust. Soc. Am. **37**(3), 409–412 (1965).
[49]ISO 3382:1997(E): *Acoustics—Measurement of the Reverberation Time of Rooms with Reference to Other Acoustical Parameters* (International Organization for Standardization, Geneva, Switzerland, 1997).
[50]M. H. Denison and B. E. Anderson, "The effects of source placement on time reversal focusing in rooms," Appl. Acoust. **156**, 279–288 (2019).
[51]T. Jenny and B. E. Anderson, "Ultrasonic anechoic chamber qualification: Accounting for atmospheric absorption and transducer directivity," J. Acoust. Soc. Am. **130**(2), EL69–EL75 (2011).
[52]B. D. Patchett, B. E. Anderson, and A. D. Kingsley, "The impact of room location on time reversal focusing amplitudes," J. Acoust. Soc. Am. **150**(2), 1424–1433 (2021).
[53]N. Roy, H. Hassanieh, and R. R. Choudhury, "BackDoor: Making microphones hear inaudible sounds," in *MobiSys. '17*, Niagara Falls, NY (June 19–23, 2017), pp. 2–14.
[54]C. Ye, Z. Kuang, M. Wu, and J. Yang, "Development of an acoustic filter for parametric loudspeaker in air," Jap. J. Appl. Phys. **50**(7), 07HE18 (2011).
[55]P. Ji and J. Yang, "An experimental investigation about parameters' effects on spurious sound in parametric loudspeaker," Appl. Acoust. **148**, 67–74 (2019).
[56]M. Griffa, B. E. Anderson, R. A. Guyer, T. J. Ulrich, and P. A. Johnson, "Investigation of the robustness of time reversal acoustics in solid media through the reconstruction of temporally symmetric sources," J. Phys. D. Appl. Phys. **41**(8), 085415 (2008).
[57]M. Scalerandi, M. Griffa, and P. A. Johnson, "Robustness of computational time reversal imaging in media with elastic constant uncertainties," J. Appl. Phys. **106**(11), 114911 (2009).